

GALACTIC CEPHEIDS AS TRACERS OF THE THIN DISK IN THE GAIA AREA

B. Lemasle¹, H. N. Lala¹, V. Kovtyukh², M. Hanke¹, Z. Prudil¹, G. Bono^{3,4}, V. F. Braga^{4,5}, R. da Silva^{4,5}, M. Fabrizio^{4,5}, G. Fiorentino⁴, P. Francois^{6,7}, E. K. Grebel¹ and A. Kniazev^{8,9,10}

Abstract. Since the Sun is located in the Galactic plane and because of interstellar extinction, mapping the structure of the Galactic disk is a difficult task. In a recent paper, we investigated the properties of the Milky Way warp and spiral arms using Cepheids. Indeed, they are bright stars and can thus be observed at large distances, and their distances are known with great accuracy thanks to period-luminosity relations. With a robust regression method, we derived the parameters of the warp. Once the Cepheids' distances corrected from the (small) effects of the warp, we identified groups of Cepheids as segments of spiral arms using a clustering algorithm. These groups are consistent with previous studies determining the location of the spiral arms directly from young tracers (masers, OB(A) stars) or mapping overdensities of upper main-sequence stars in the Solar neighborhood.

Keywords: Stars: variables: Cepheids, Galaxy: disk, Galaxy: structure

1 Introduction

Cepheids are massive/intermediate-mass pulsating variable stars whose distances are known with great accuracy thanks to their period-luminosity relations. Their ages do not exceed a few hundreds of megayears, making them excellent tracers of young stellar populations. Regarding the Galactic structure, they have been used to derive the Galactocentric distance of the Sun and to determine the Milky Way rotation curve (e.g., Caldwell & Coulson 1987; Pont et al. 1997; Metzger et al. 1998; Mróz et al. 2019, and references therein) or to trace the Galactic warp (Chen et al. 2019; Dékány et al. 2019; Skowron et al. 2019a,b). Only recently, Dambis et al. (2015) matched their sample of Cepheids to a four-armed pattern with a pitch angle of $9.5 \pm 0.1^\circ$, while Minniti et al. (2021) found them compatible instead with a two-arms model expanding into four arms for $R_G \gtrsim 5\text{--}6$ kpc.

2 Catalog

A catalog of classical Cepheids has been built by robustly cross-matching all candidates and confirmed Cepheids from photometric surveys with time-domain capabilities against *Gaia* EDR3. For *Gaia* astrometric and photometric data, large-scale systematics, binarity, or crowded regions were taken into account following the recommendations found in the literature (Fabricius et al. 2021; Lindegren et al. 2021; Riello et al. 2021).

We derived a new period-Wesenheit relation in the W1, W2 WISE bands using a Bayesian robust regression computed with `pymc3` (Salvatier et al. 2016). It was calibrated on Large Magellanic Cloud (LMC) Cepheids

¹ Astronomisches Rechen-Institut, ZAH, Universität Heidelberg, Mönchhofstr. 12-14, D-69120 Heidelberg, Germany

² Astronomical Observatory, Odessa National University, Shevchenko Park, UA-65014 Odessa, Ukraine

³ Dipartimento di Fisica, Università di Roma Tor Vergata, via della Ricerca Scientifica 1, I-00133 Rome, Italy

⁴ INAF - Osservatorio Astronomico di Roma, via Frascati 33, Monte Porzio Catone, I-00078 Rome, Italy

⁵ Agenzia Spaziale Italiana, Space Science Data Center, via del Politecnico snc, I-00133 Rome, Italy

⁶ GEPI, Observatoire de Paris, CNRS, Université Paris Diderot, Place Jules Janssen, 92190, Meudon, France

⁷ UPJV, Université de Picardie Jules Verne, 33 rue St. Leu, 80080, Amiens, France

⁸ South African Astronomical Observatory, PO Box 9, 7935 Observatory, Cape Town, South Africa

⁹ Southern African Large Telescope Foundation, PO Box 9, 7935 Observatory, Cape Town, South Africa

¹⁰ Sternberg Astronomical Institute, Lomonosov Moscow State University, Universitetskij Pr. 13, Moscow 119992, Russia

using the LMC distance modulus (18.477 mag) from Pietrzyński et al. (2019). It relies on unWISE photometry (Meisner et al. 2021), which consists of all-sky static coadds based on six years of WISE and NEOWISE operations, with an improved treatment of crowded regions. Period-luminosity relations in the near-infrared provide more accurate distances because i) their intrinsic dispersion is reduced, ii) their metallicity-dependence is very weak (if any), iii) reddening itself is also reduced. In addition, Wesenheit pseudo-magnitudes are unaffected by the extinction toward individual stars (or their uncertainties) by construction (Madore 1982), leaving a possible nonuniversality of the reddening law as the only notable uncertainty.

However, WISE photometry is sometimes missing, in particular for the nearby Cepheids because they are too bright. We then used as distance the inverse of the *Gaia* EDR3 parallax, provided this distance is less than 5 kpc. To avoid Cepheids with spurious astrometric solutions, we considered only stars with a fractional parallax uncertainty < 0.33 . The maximum limit for the fractional parallax uncertainty is usually set at 0.15; we noticed however that the agreement between parallax-based distances and those derived from various period-Wesenheit relations remains good enough (median difference ~ 0.6 kpc) to allow for this extension.

Furthermore, we limited ourselves to Cepheids pulsating in the fundamental (F) or the first-overtone (1O) mode as their ages can be derived from period-age relations. We ended up with a catalog containing 2684 (F,1O) Cepheids (2098 with WISE-based distances, 586 with *Gaia* parallax-based distances), while the catalogs of Chen et al. (2019) and Skowron et al. (2019b) contained 1339 and 2390 Cepheids, respectively. Details regarding the catalog can be found in Lala et al., in prep.

3 The Galactic warp

The Galactic warp (Kerr 1957; Oort et al. 1958) is a large-scale perturbation of the Milky Way disk, caused by a torque exerted on the disk, and whose origin is still lively debated. We estimated the parameters of the warp model using a Bayesian robust regression method. For the likelihood of the model, we retained the warp formula by Skowron et al. (2019b) given in Eq. 3.1: the warp starts at a r_0 radius, where r is the distance from the Galactic center. Θ is the Galactocentric azimuth, with $\Theta=180^\circ$ pointing toward the Galactic anticenter, and z is the vertical distance from the Galactic plane. We assumed a Student's t -distribution for the likelihood, because it is much less sensitive to outliers than, for instance, a normal distribution. Unlike previous studies, we accounted for uncertainties on (r, Θ, z) and their covariances, they were propagated from the uncertainties and covariances on right ascension, declination, and distances using Jacobian matrices (ESA 1997; Price-Whelan 2017) to perform coordinates transformations. However, the uncertainties on the position of the Sun relative to the Galactic center have been ignored. We used the Hamiltonian MCMC sampler (Betancourt 2017) of `pymc3` to sample the posterior distributions. We adopted the mean values and the standard deviations of the posterior distributions as the parameters of the warp and their uncertainties, respectively. They can be found in Lemasle et al. (2022), together with the full covariance matrix.

$$z(r, \Theta) = \begin{cases} z_0 & r < r_0 \\ z_0 + (r - r_0)^2 \times [z_1 \sin(\Theta - \Theta_1) + z_2 \sin(2(\Theta - \Theta_2))] & r \geq r_0 \end{cases} \quad (3.1)$$

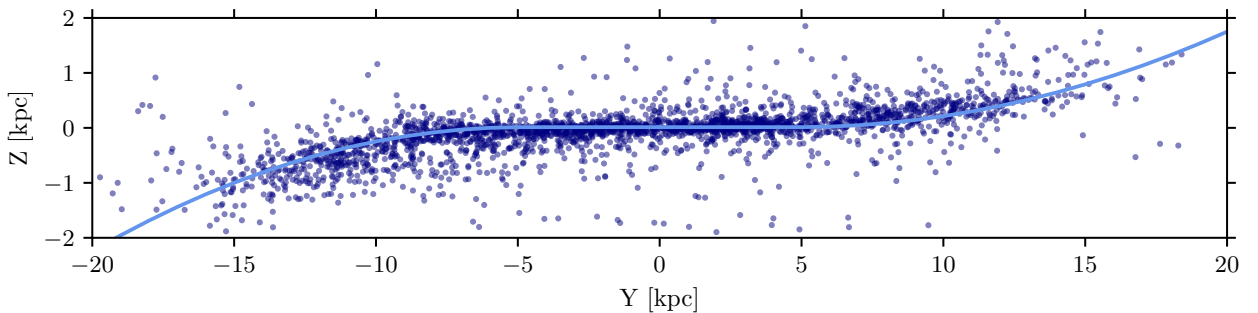


Fig. 1. Milky Way warped disk (light blue) computed for $X=0$ kpc (see Fig. 2), that is, the diameter perpendicular to the Sun–Galactic center direction. The warp parameters were determined with a robust regression method. Individual Cepheids are overplotted in dark blue.

Our results are in excellent agreement with those from Skowron et al. (2019b), mainly because these are the two studies with the largest number of Cepheids. Our results are also in excellent agreement with those based on HI, for instance, Nakanishi & Sofue (2003), and especially Levine et al. (2006) and Kalberla et al. (2007). A comparison (at the same Galactocentric distance) of the warp altitudes reached by various tracers above and below the Galactic plane indicates that the warp becomes more pronounced when following older tracers (see, e.g., Romero-Gómez et al. 2019). We note that the scale of the Z-axis is inflated in Fig. 1; in fact, differences between Cepheids' Galactocentric distances computed either on a flat or on a warped disk are negligible. They cannot account for the somewhat larger dispersion of abundance gradients reported by several authors in the outer disk (Lemasle et al. 2008; Genovali et al. 2014).

4 The Milky Way spiral structure

Since tracers evolve off the spiral arms once they are born, investigating the spiral structure requires selecting truly young tracers (H II regions, O stars), or considering only the youngest objects for tracers spanning a larger age range (Cepheids, open clusters). Maser sources located in high-mass star-forming regions are one of the best tracers available: they are very young, their parallaxes can be measured with radio-interferometry (Reid et al. 2019) but only a few hundreds are known so far. Other very young tracers are numerous enough (for instance, H II regions, Georgelin & Georgelin 1976), but their distances rely on kinematical models. Thanks to Gaia parallaxes, that remain accurate up to ≈ 5 kpc, a clearer picture of the spiral structure in the Solar neighborhood has emerged using OB(A) stars (e.g., Poggio et al. 2021; Zari et al. 2021) or young open clusters (e.g., Castro-Ginard et al. 2021; Hao et al. 2021) as tracers.

In order to locate the spiral arms, we used \mathbf{t} -SNE (t-distributed Stochastic Neighbor Embedding, van der Maaten & Hinton 2008) in the $(\theta, \ln r)$ coordinates space, where r was corrected from the effects of the warp. We then used the clustering algorithm HDBSCAN (Campello et al. 2015; McInnes et al. 2017) to identify groups in the \mathbf{t} -SNE output space. Tests on a mock spiral structure based on the Reid et al. (2019) model have shown that the mock spiral arms are very well recovered, even with large numbers of "inter-arm" Cepheids, that can be considered as noise. The algorithm is sensitive to small gaps within individual arms, which may split the given arm into several segments. When two spiral arms are close to each other, the algorithm might wrongly join two segments from different arms into an artificial structure. Arbitrarily, we considered only Cepheids younger than 150 Myr, a compromise to keep a relatively large sample without including objects that may have drifted too far away from their birthplace.

Fig. 2 indicates that the segments of spiral recovered by the algorithm are consistent with previous studies deriving explicitly the location of the spiral arms (Reid et al. 2019; Hou 2021) or mapping the density of young stellar tracers in the vicinity of the Sun (Poggio et al. 2021; Zari et al. 2021). From a much smaller sample of Cepheids covering a restricted range of azimuths, Veselova & Nikiforov (2020) also identified sections of a logarithmic spiral arms using an independent method. The Galactocentric distances of the spiral arms in their study and in ours are in very good agreement, suggesting that our detection of spiral arms is robust. The agreement is also fairly good with the groups of Cepheids identified by Genovali et al. (2014), who used a Path Linkage Criterion clustering algorithm (Battinelli 1991) without considerations on age.

5 Conclusions

Thanks to an updated catalog of Galactic Cepheids, we determined the shape of the Milky Way warp using a Bayesian robust regression method, we concluded that the warp cannot be responsible for the increased dispersion of abundance gradients in the outer disk. Using a clustering algorithm, we identified groups of Cepheids which can be considered as portions of spiral arms. They are consistent with previous studies mapping the density of young tracers in the Solar neighborhood or deriving explicitly the location of the spiral arms.

References

- Battinelli, P. 1991, *A&A*, 244, 69
 Betancourt, M. 2017, arXiv e-prints, arXiv:1701.02434
 Caldwell, J. A. R. & Coulson, I. M. 1987, *AJ*, 93, 1090
 Campello, R. J. G. B., Moulavi, D., Zimek, A., & Sander, J. 2015, *ACM Trans. Knowl. Discov. Data*, 10
 Castro-Ginard, A., McMillan, P. J., Luri, X., et al. 2021, *A&A*, 652, A162

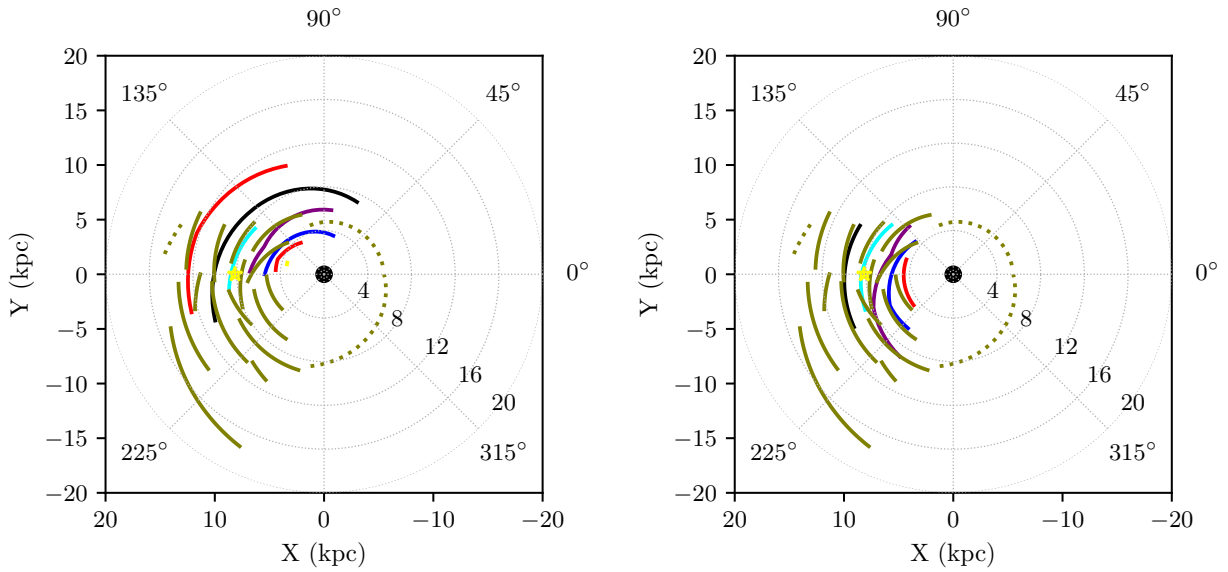


Fig. 2. Comparison with previous models. *Left:* Recovered spiral segments (olive) and the model of Reid et al. (2019). The spiral arms delineated by Reid et al. (2019) are shown with the same color-coding as in the original paper. *Right:* Recovered spiral segments (olive) and the model of Hou (2021), with the same color-coding as in Reid et al. (2019).

- Chen, X., Wang, S., Deng, L., et al. 2019, *Nature Astronomy*, 3, 320
- Dambis, A. K., Berdnikov, L. N., Efremov, Y. N., et al. 2015, *Astronomy Letters*, 41, 489
- Dékány, I., Hajdu, G., Grebel, E. K., & Catelan, M. 2019, *ApJ*, 883, 58
- ESA. 1997, *ESA Special Publication*, 1200
- Fabrizius, C., Luri, X., Arenou, F., et al. 2021, *A&A*, 649, A5
- Genovali, K., Lemasle, B., Bono, G., et al. 2014, *A&A*, 566, A37
- Georgelin, Y. M. & Georgelin, Y. P. 1976, *A&A*, 49, 57
- Hao, C. J., Xu, Y., Hou, L. G., et al. 2021, *A&A*, 652, A102
- Hou, L. G. 2021, *Frontiers in Astronomy and Space Sciences*, 8, 103
- Kalberla, P. M. W., Dedes, L., Kerp, J., & Haud, U. 2007, *A&A*, 469, 511
- Kerr, F. J. 1957, *AJ*, 62, 93
- Lemasle, B., François, P., Piersimoni, A., et al. 2008, *A&A*, 490, 613
- Lemasle, B., Lala, H. N., Kovtyukh, V., et al. 2022, *arXiv e-prints*, arXiv:2209.02731
- Levine, E. S., Blitz, L., & Heiles, C. 2006, *ApJ*, 643, 881
- Lindgren, L., Klioner, S. A., Hernández, J., et al. 2021, *A&A*, 649, A2
- Madore, B. F. 1982, *ApJ*, 253, 575
- McInnes, L., Healy, J., & Astels, S. 2017, *The Journal of Open Source Software*, 2, 205
- Meisner, A. M., Lang, D., Schlafly, E. F., & Schlegel, D. J. 2021, *Research Notes of the American Astronomical Society*, 5, 168
- Metzger, M. R., Caldwell, J. A. R., & Schechter, P. L. 1998, *AJ*, 115, 635
- Minniti, J. H., Zoccali, M., Rojas-Arriagada, A., et al. 2021, *A&A*, 654, A138
- Mróz, P., Udalski, A., Skowron, D. M., et al. 2019, *ApJ*, 870, L10
- Nakanishi, H. & Sofue, Y. 2003, *PASJ*, 55, 191
- Oort, J. H., Kerr, F. J., & Westerhout, G. 1958, *MNRAS*, 118, 379
- Pietrzyński, G., Graczyk, D., Gallenne, A., et al. 2019, *Nature*, 567, 200
- Poggio, E., Drimmel, R., Cantat-Gaudin, T., et al. 2021, *A&A*, 651, A104
- Pont, F., Quéloz, D., Bratschi, P., & Mayor, M. 1997, *A&A*, 318, 416
- Price-Whelan, A. M. 2017, *The Journal of Open Source Software*, 2

- Reid, M. J., Menten, K. M., Brunthaler, A., et al. 2019, *ApJ*, 885, 131
- Riello, M., De Angeli, F., Evans, D. W., et al. 2021, *A&A*, 649, A3
- Romero-Gómez, M., Mateu, C., Aguilar, L., Figueras, F., & Castro-Ginard, A. 2019, *A&A*, 627, A150
- Salvatier, J., Wiecki, T. V., & Fonnesbeck, C. 2016, *PeerJ Computer Science*, 2, e55
- Skowron, D. M., Skowron, J., Mróz, P., et al. 2019a, *Science*, 365, 478
- Skowron, D. M., Skowron, J., Mróz, P., et al. 2019b, *Acta Astron.*, 69, 305
- van der Maaten, L. & Hinton, G. 2008, *Journal of Machine Learning Research*, 9, 2579
- Veselova, A. V. & Nikiforov, I. 2020, *Research in Astronomy and Astrophysics*, 20, 209
- Zari, E., Rix, H. W., Frankel, N., et al. 2021, *A&A*, 650, A112